Available online www.ejaet.com

European Journal of Advances in Engineering and Technology, 2016, 3(7): 1-8

Research Article ISSN: 2394 - 658X

On the Introduction of the Irreversibility in a DBD Plasma Based Channel Flow: A Study on Entropy Generation Rate

A Jafarimoghaddam[1] and S Aberoumand[2]

[1]*Department of Aerospace Engineering, K. N. Toosi University of Technology, Tehran, Iran*
[2]*Department of Mechanical Engineering, Islamic Azad University, Takestan, Iran*
a.jafarimoghaddam@gmail.com

ABSTRACT

In the present research, a brief study on the impact of DBD (Dielectric Barrier Discharge) plasma actuator on the entropy generation rate in a channel flow is presented. The work has been continued in the certain inlet Reynolds number of about 670. Moreover, the problem is assumed to be a two dimensional DBD plasma based channel flow with the assumption of the incompressible flow. Since, the distribution of entropy generation rate is governed by a contribution of temperature and velocity gradients, and besides, the distribution of DBD plasma body force is highly depended on the channel width and other parameters of the actuator configuration, it would be difficult to include the whole engaged effects together for pursuing the study of entropy generation rate in a plasma based channel flow. So the present work aims to provide an over view on this problem. Therefore, for a certain channel geometry and inlet Reynolds number and different DBD plasma configurations, entropy generation rate and Bejan number is studied.

Key words: DBD plasma actuators, Entropy generation rate, Plasma based channel flow, Numerical model, Bejan number in the presence of DBD plasma actuator

---

INTRODUCTION

The applications of Electoro- Hydrodynamics have been very vast in the last decades. Electro- magnetic force has been employed for many purposes including the flow and particle control. Two sorts of electro- magnetic force have been conventional so far. First is the Corona plasma wind, which is applied by DC power supply and is usually applicable for the process of mixing the fluid flow, ESP (Electro- Static Precipitator) and etc. the second one is DBD plasma actuator, which is applied by AC power supply and is usually used for the flow control process [1- 4]. Using the electric field for flow control has been reviewed by Cattefesta and Sheplak [5]. Plasma actuator has been tested in variety of applications [6-14] including channel flows [15- 17] and it has been observed that the actuator causes a body force field which is directed from the exposed electrode to the encapsulated one. So, this last decade has been an exhibition of the variety of applications of DBD plasma body force [7-8]. Because experimental investigations of DBD plasma actuator are so expensive, CFD tools can be applied for discovering the nature of such an actuator in different applications. Considering this that the DBD plasma actuator works in a semi- steady mode, it is inferred that it could be possible to decouple plasma equation with Navier- Stokes equations and then substituting the solution of plasma body force as the source term into the Navier- Stokes equations. Coming to the numerical models for predicting the DBD plasma body force, Lumped Circuit Element Electro- Static and Suzen Huang stand as the most prominent models for predicting the body force of the DBD plasma actuator [15]. Lumped Circuit Element is an auxiliary model which associates with the Single Potential Model (Electro- Static Model with considering a relation between the charge density and electric potential). This model can simply modify the basic Electro- Static model by considering this that air and dielectric are capacitor elements. So each path line from the exposed to the covered dielectric is comprised of a sub- circuit which is set as to be parallel with the others. This model can predict the location of the presence of charge timely. So the Poisson equation for potential electric is solved in this location rather than to be solved in the whole region over the encapsulated electrode 2016 [18]. The other advantage of this model is to consider the effect of applied voltage frequency on DBD plasma body force and also this model allows us to calculate the plasma dissipation. Since, Aberoumand *et al* [18] suggested that it could be possible to use this plasma dissipation as a thermal flux on the

virtual electrode (surface of the dielectric), so this model (Lumped Circuit Element Electro- Static) has a privilege in applications for thermal problems. By taking this advantage of the model, the temperature distribution in the presence of DBD plasma actuator in different actuator configurations can simply be quantified. Note that in low pressure plasma actuators, the drift diffusion can be ignored by having this fact that the collision between the electrons and the neutral air is relatively low. So the energy of electrons cannot be easily transferred to the gas (neutral air), so there would not be a temperature equilibrium between the electrons and the neutral air. Therefore the neutral gas is in a considerably different temperature than the electrons and consequently the energy diffusivity is not needed to be included for the solution of the plasma formation phenomenon. So, it can be concluded that considering the plasma formation as a cold plasma classification (low pressure plasma actuator), there is not a route to simulate the gas temperature distribution while the energy diffusivity is ignored in the proposed models for the simulation of DBD plasma actuator. So, in the present work, by using the methodology for simulating the Thermal effect of the actuator proposed in 2016 [18], the study has been continued. Although DBD plasma actuators are studied in many applications so far but the manipulation of entropy generation rate and also Bejan number are not yet comprehensively studied in the literature of these actuators. Therefore the goal of the investigation is to use the obtained temperature field (caused by DBD plasma actuator) to calculate the entropy generation rate and also Bejan number. The present research aims to introduce the manipulation of these parameters (entropy generation rate and Bejan number). The changes in entropy generation rate and Bejan number by using DBD plasma actuator is shown here to be significant and considerable for related applications. As it was previously mentioned, we have continued the present simulation in a constant inlet Reynolds number and a fixed geometry while the configuration of the DBD plasma actuator was changed during the study. We have also considered the parameters of applied voltage frequency, dielectric coefficient, electrodes length and vertical and horizontal distances between them, constant, while the DBD plasma configuration was changed by changing the peak voltage amplitude. Since in this study, there are many parameters that were assumed constant, further researches are still required to decipher the manipulation of entropy generation rate and Bejan number in the presence of DBD plasma actuator.

DBD PLASMA MODEL

In general, DBD plasma actuator can be modelled by Electro- Static Model [19]. So, in the present work, we have only brought up the main governing equations.
Electrical potential is governed by the following Poisson equation [19]:

$$\nabla(\varepsilon\nabla\varphi)=\frac{1}{\lambda_D^2}\varphi \tag{1}$$

The charge density is obtained from the one- dimensional simulation of the electric charge [19] as:

$$\rho_c=-\frac{\varepsilon_0}{\lambda_D^2}\varphi. \tag{2}$$

By presenting the net charge in a region with the presence of electric field, the induced body force by the DBD plasma actuator can be obtained by:

$$\overrightarrow{f_b}=\rho_C\overrightarrow{E}. \tag{3}$$

NUMERICAL FORMULATION OF MODIFIED ELECTRO-STATIC LUMPED CIRCUIT ELEMENT MODEL

In general, the electro- static model for DBD plasma actuator deals with solving Eq. (1) in a mathematical plain, obtaining induced body force due to the presence of the plasma actuator and then mapping the domain into the physical space of the problem. Since Lumped Circuit Element model, is an approach in which considers electrodes, air and dielectric as capacitor elements and each element as finite numbers of attached sectors (subscripted by n), then first, for modifying the Electro- Static model, the modified spatial-time Lumped Circuit Element model, discussed in [19], was used in order to obtain the region of the presence of plasma temporally, $x(t)$, and also dielectric virtual voltage $V_n(t)$ by simultaneously solving of Eq. (4) to (6). Schematic of the model is shown in Fig.1.

$$\frac{dV_n(t)}{dt}=\frac{dV_{app}(t)}{dt}\left(\frac{C_{an}(t)}{C_{an}(t)+C_{dn}(t)}\right)+k_n\frac{I_{pn}(t)}{C_{an}(t)+C_{dn}(t)} \tag{4}$$

$$I_{pn}(t)=\frac{1}{R_n}[V_{app}(t)-V_n(t)] \tag{5}$$

$$\frac{dx(t)}{dt}=\nu v\left|V_{app}(t)-V_n(t)\right| \tag{6}$$

In which $\nu\nu$, is a coefficient representing the increase in the sweep velocity by the increase of applied voltage amplitude. According to [19], $\nu\nu$ is assumed to be $10\frac{m/s}{kV}.V_{app}(t)$, represents the applied voltage amplitude, $V_n(t)$ is the voltage at the virtual electrode in each sector of the encapsulated electrode which is assumed to be on the surface of dielectric material, $I_{pn}(t)$ is the current through the plasma resistance for each sector, R_n is the air resistance in each section, C_{an} and C_{dn} are capacitor elements of air and dielectric respectively, and k_n is a constant which is assumed to be 0 or 1 depending on the presence of plasma in the each sector. These factors are well discussed in [19]. Equations of 4 to 6 were solved by using forth order Range-Kutta. Then, Eq. 1 was solved for spatial-time re-corrected conditions. Finally the obtained spatial steady body force was substituted into the Navier-Stokes equations as the source term. Length of the exposed and encapsulated electrodes was assumed to be 0.5inch for both and also in the present work, vertical and horizontal distances between the electrodes were assumed to be 0.003 inch [19]. Based on the results of the present simulation by Electro- Static Model, plasma is formed just on a region over the encapsulated electrode. This happens because there would be no assumption of the presence of charge density in other regions in this model. Moreover, it is noticeable that vertical body force is almost negligible in comparison with the horizontal body force. So, according to the results of the present simulation, the vertical term of the body force contains less than 10% of the horizontal body force for each case. As the result of this simulation by Lumped Circuit Element Electro- Static Model, the plasma body force for the case of having the applied voltage frequency of 10 KHz and peak voltage amplitude of 5.5 KV is shown in Fig. 2. Other cases possess a similar body force distribution shape (this is maybe because of changing only the peak voltage amplitude in each case) and the difference is only in the range of the distribution. So, the result of other cases is provided in Table 1. This Table shows the maximum induced body force for each case. One of the advantages of modelling DBD plasma actuator by Modified Lumped Circuit Element is the possibility of simulating the plasma dissipation by the following equation:

$$P_n(t) = I_{pn}(t)[V_{app}(t) - V_n(t)] \tag{7}$$

In fact, plasma dissipation stands as a term which demonstrates the power loss by the DBD plasma actuator. And furthermore, this power almost losses from the surface of the dielectric. The whole power loss for DBD plasma actuator (P(W)) can be obtained by summing the $P_n(t)$ for any sector of virtual electrode. The results of simulation for DBD plasma dissipation is also provided in Table 2. In the present simulation, the minimum voltage required for ionization (formation of plasma) is assumed to be 1KV based on the previous work in [19]. And this can be considered as another simplification in the simulation of DBD plasma actuator.

Table -1 Maximum Induced Body Force in Different Peak Voltage Amplitudes

Peak Voltage Amplitude (V)	Maximum Induced Body Force (N/ m^3)
1500	9.1698
2000	20.6418
2500	36.7038
3000	57.357
3500	82.626
4000	112.4358
4500	146.8614
5000	185.877
5500	229.4844

Table -2 The Whole Power Loss for DBD Plasma Actuator in Different Peak Voltage Amplitudes

Peak Voltage Amplitude (V)	P(W)
1500	15
2000	17
2500	18.7
3000	19.3
3500	20.5
4000	22
4500	23.5
5000	25
5500	26.3

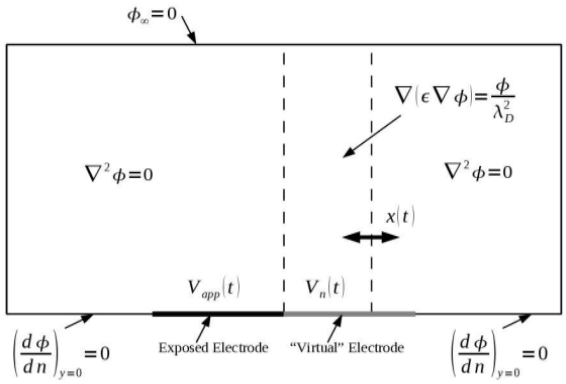

Fig.1 Lumped Circuit Element Electro- Static model [19]

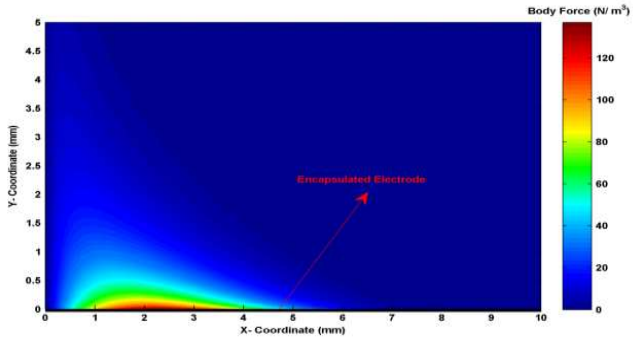

Fig. 2 DBD Plasma body force

Plasma Validation

A comparison between experimental measurements reported by Debiasi *et al* [17] at threshold voltage of 12 KV, 25000Hz for the voltage frequency and Kapton as the dielectric in conditions and specific plasma configuration used in the experiment, and the present numerical simulation is shown in Fig.3. It is illustrated that the simulated plasma is in a good agreement with the experiment. In this case, Debye length was chosen to be 0.00001 based on the previous work by Ibrahim *et al* [15].

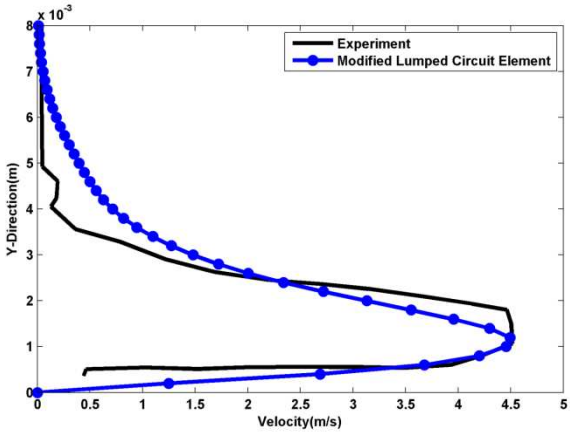

Fig.3 Comparison between experimental results reported in [17] and numerical simulation in this study

Fluid Flow Equations

For 2D incompressible flows, the governing equations can be denoted as continuity, momentum and energy equations. The presence of DBD plasma results in the presence of body force term in the right hand side of the momentum equations. So, the governing equations can be written as:

Continuity:

$$\frac{\partial u}{\partial x}+\frac{\partial v}{\partial y}=0 \tag{8}$$

Momentum:

$$\begin{aligned}\rho(u\frac{\partial u}{\partial x}+v\frac{\partial u}{\partial y})&=-\frac{\partial p}{\partial x}+\mu(\frac{\partial^2 u}{\partial x^2}+\frac{\partial^2 u}{\partial y^2})+f_{bx}(x,y)\\ \rho(u\frac{\partial v}{\partial x}+v\frac{\partial v}{\partial y})&=-\frac{\partial p}{\partial y}+\mu(\frac{\partial^2 v}{\partial x^2}+\frac{\partial^2 v}{\partial y^2})+f_{by}(x,y)\end{aligned} \tag{9}$$

Energy:

$$c_p(u\frac{\partial T}{\partial x}+v\frac{\partial T}{\partial y})=k(\frac{\partial^2 T}{\partial x^2}+\frac{\partial^2 T}{\partial y^2})+\phi \tag{10}$$

In Eq. (10), φ is the dissipation term which is defined as:

$$\phi=\mu\left[2(\frac{\partial u}{\partial x})^2+2(\frac{\partial v}{\partial y})^2+(\frac{\partial u}{\partial y}+\frac{\partial v}{\partial x})^2\right] \tag{11}$$

Moreover $f_{bx}(x,y)$ and $f_{by}(x,y)$ are the horizontal and vertical components of the DBD plasma body force respectively.

The above equations are solved for the variety of DBD plasma configurations using ANSYS Fluent 16.0.

Finally, the entropy generation rate and Bejan number can be obtained by using the following equations:

$$\dot{s}_{gen}=\frac{k}{T^2}\left[(\frac{\partial T}{\partial x})^2+(\frac{\partial T}{\partial y})^2\right]+\frac{k}{T}\left[2(\frac{\partial u}{\partial x})^2+2(\frac{\partial v}{\partial y})^2+(\frac{\partial u}{\partial y}+\frac{\partial v}{\partial x})^2\right] \tag{12}$$

$$Be=\frac{(k/T^2)[(\partial T/\partial x)^2+(\partial T/\partial y)^2]}{\dot{S}_{gen}} \tag{13}$$

In the present work, the whole figures (acquired data of the simulation) have been visualized by MATLAB.

SCHEMATIC OF THE PROBLEM AND MESH INDEPENDENCY

For a 2D and incompressible DBD plasma based channel flow, the schematic of the problem which was used in the present study is drawn in Fig. 4.

As it can be seen from the schematic of the problem, we have assumed the actuator (DBD plasma) just placed at the inlet of the channel flow. Moreover, the inlet velocity was considered to be uniform in low Reynolds number of about 670. Furthermore, the temperature of the entire boundaries of the simulated channel flow is assumed to be constant at 300K. By this assumption we could make sure that the thermal effect is almost due the presence of the DBD plasma actuator. The DBD plasma actuator was configured as 10 KHz for the applied voltage frequency and Kapton as the dielectric with the dielectric coefficient of 2.8. The most challenging case (peak voltage amplitude of 5.5 KV) has been selected to check the mesh independency. So, the maximum velocity in the computational domain has been calculated in different applied grids in this case. The result of mesh independency is provided in Fig. 5.

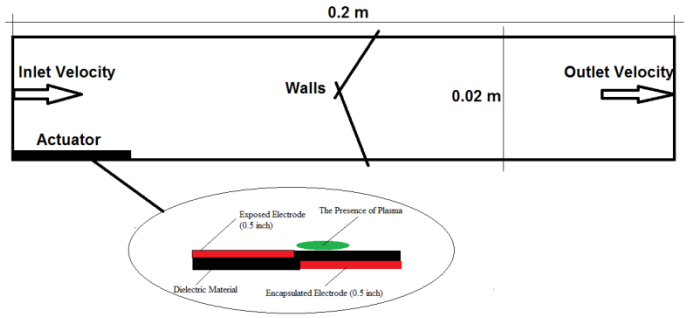

Fig. 4 The schematic of the problem

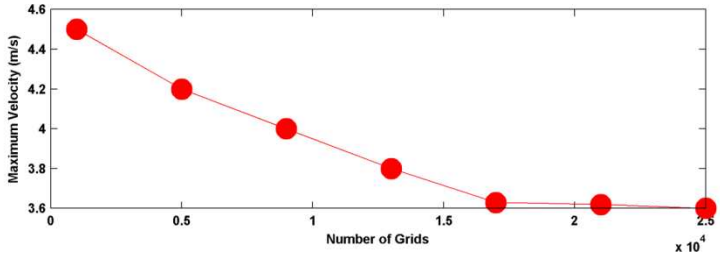

Fig. 5 Mesh independency

RESULTS AND DISCUSSION

In this section, after each part of discussion, the results are addressed. Moreover, the contours are provided for three cases of Without Plasma, Minimum Simulated Plasma (peak voltage amplitude of 1.5 KV) and Maximum Simulated Plasma (peak voltage amplitude of 5.5 KV). For other cases, the results are assembled in Tables. As it is well defined in the literature so far as the most prominent feature of DBD plasma actuators, the induced body force pulls the flow from the exposed electrode and drives it towards the encapsulated one (Fig. 6). In the case of channel flow, Ibrahim *et al* [15] showed that the width of the channel can easily interfere in the distribution of DBD plasma body force. In which if the width of the channel is selected to be less than a few milli meters, the effect of plasma body force may extend to the upper wall of the channel flow. As the result of this extension, the upper boundary layer will be manipulated as well. Since Ibrahim *et al* [15] used two actuators placed symmetrically at the top and the bottom of the channel, by decreasing the width of the channel a collision between the induced body forces by the two actuators was observed at the middle of the channel. In the present research in order to be sure of this that the induced DBD plasma body force does not extend to the upper wall of the channel, the width of the channel flow was chosen to be high enough in which in the most challenging case (peak voltage amplitude of 5.5 KV as it was previously shown in Fig. 2) the total induced plasma body force is almost obscured in 5mm above the actuator. Based on the previous work by Aberoumand *et al* [18], the term of plasma dissipation is assumed as the thermal flux condition just on the virtual electrode (on the surface of the dielectric material). By using this assumption, the distribution of temperature in the presence of DBD plasma actuator is obtained. This temperature distribution is compared in the three cases of Without Plasma, Minimum Simulated Plasma and Maximum Simulated Plasma Fig. 7- 9. In the case of Without Plasma, the difference of the temperature in the domain is certainly due to the dissipation term in the energy equation. Since this term is almost negligible, it was simply seen from the results of the present simulation that even by having the considerable velocity gradients caused by the DBD plasma actuator, the differences in the temperature in the whole computational domain does not exceed a few degrees. The entropy generation rate is governed by the impact of two major factors. First is the temperature gradients and the second is the velocity gradients (related to the dissipation term in energy equation). Considering this fact that by assuming the

thermal effect of the actuator as the thermal flux boundary on the virtual electrode (dielectric material) and having this that the energy equation in incompressible flows is in a transport form, the most temperature gradient occurs just near the actuator (encapsulated electrode) and then it would be rapidly obscured by a few centimetres further than the actuator. Furthermore, the dissipation term (velocity gradients) in a channel flow occurs mainly into the boundary layers. For the certain Reynolds number of about 670 which was assumed in the present work, the value of this term is not too high but it gets high by using the DBD plasma actuator. By applying the DBD plasma actuator the hydrodynamic boundary layer will be completely manipulated in which the most velocity gradients occur just near the actuator. As Zexiang Li *et al* [16] represented a DNS simulation of the DBD plasma based channel flow; they reported that velocity gradients in plasma based channel flow decrease rapidly by getting further from the actuator location. So both of the temperature gradients and the velocity gradients decrease quickly by passing from the DBD plasma location. Therefore, it is obvious that the contribution of these two effects simply results in the same behaviour for entropy generation rate as well Fig. 10 and 11 (note that for the case of without plasma, this entropy generation is almost zero). Coming to this point that temperature and velocity gradients occur in thermal and velocity boundary layers respectively, it can be concluded that the behaviour of entropy generation rate is governed by the simultaneous effects of the manipulation of thermal and hydrodynamic boundary layers. For Bejan number, the problem gets more complicated since this factor is defined for measuring the influence of heat transfer irreversibility and viscous dissipation in the magnitude of entropy generation. By changing the value of the peak voltage amplitude, the growth and magnitude of these two boundaries (thermal and hydrodynamic) will change. But according to the present numerical simulation, this changing does not occur in the same behaviour Fig. 12- 14. So since Bejan number indicates a contribution of these two effects (the manipulated thermal and viscous boundary layers by DBD plasma actuator) and knowing that the magnitude of these boundaries relies on several parameters including the peak voltage amplitude, voltage frequency, dielectric material, electrode geometries and the channel height, deciphering the exact behaviour of this factor (Bejan number) requires further researches. Finally, average entropy generation rate and Bejan number in the computational domain for each case are gathered into Table -3 and 4.

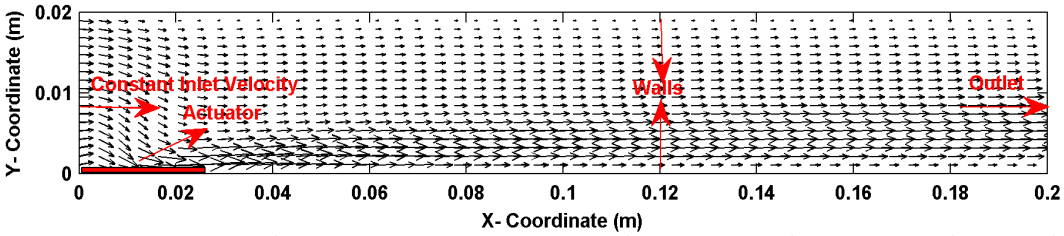

Fig. 6 Velocity vector in the presence of DBD plasma actuator: Although this figure is obtained from the results of the case of Maximum Simulated Plasma but it stands as a representative for all the present simulated cases

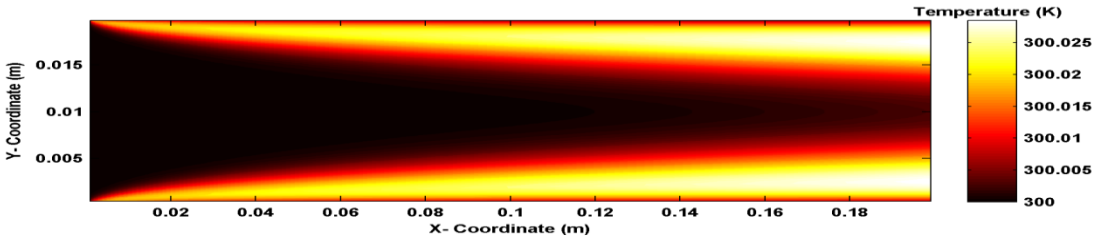

Fig.7 Temperature distribution in cases of without Plasma

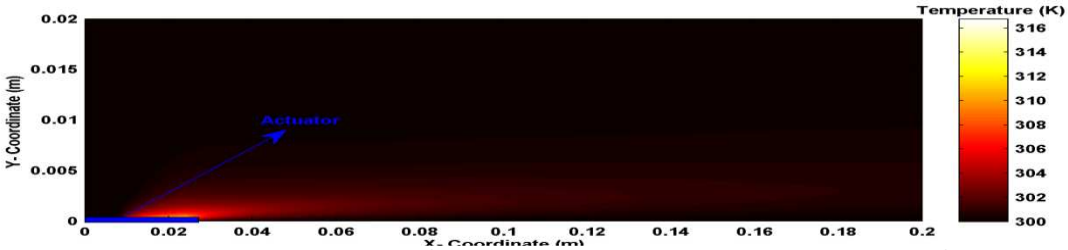

Fig.8 Temperature distribution in cases of Minimum Simulated Plasma (peak voltage amplitude of 1.5 KV)

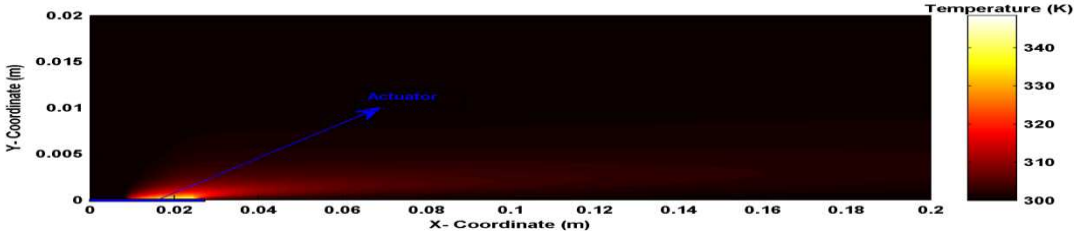

Fig.9 Temperature distribution in cases of Maximum Simulated Plasma (peak voltage amplitude of 5.5 KV)

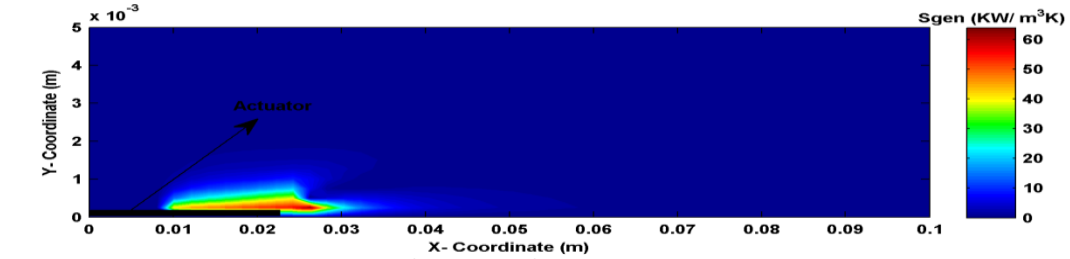

Fig. 10 Entropy generation rate for the case of Minimum Simulated Plasma (a zoomed in view)

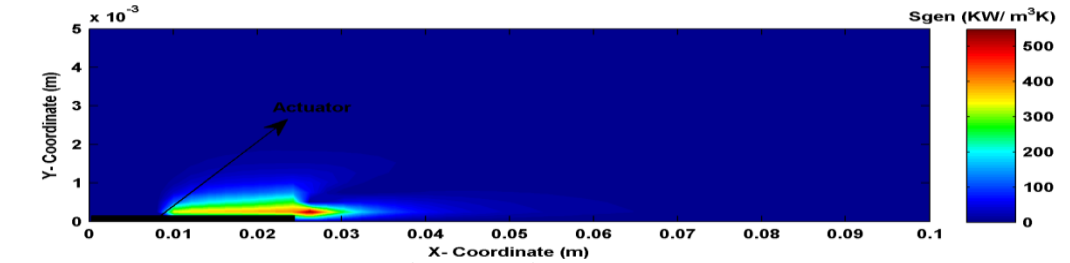

Fig. 11 Entropy generation rate for the case of Maximum Simulated Plasma (a zoomed in view)

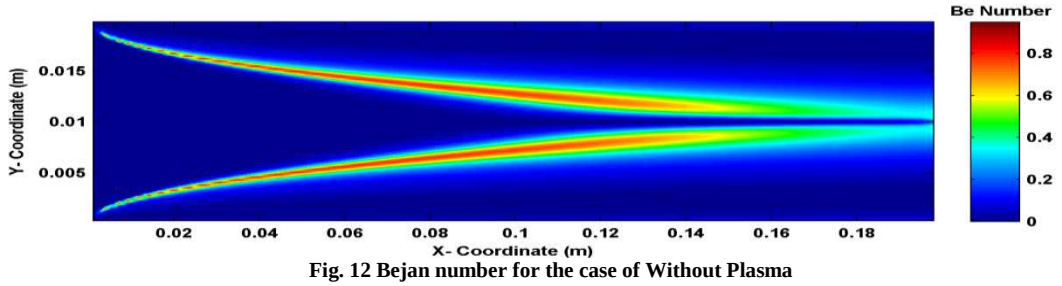

Fig. 12 Bejan number for the case of Without Plasma

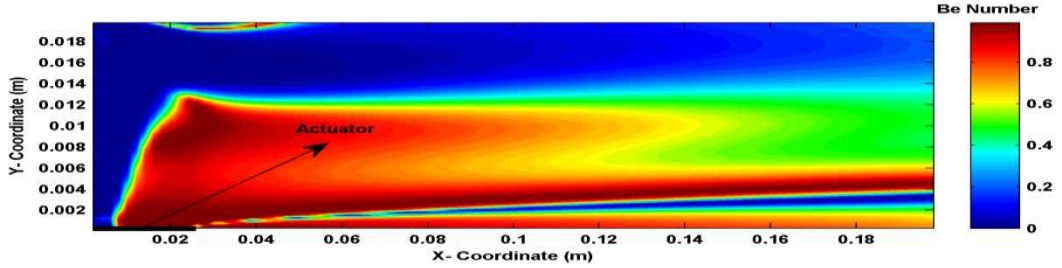

Fig. 13 Bejan number for the case of Minimum Simulated Plasma

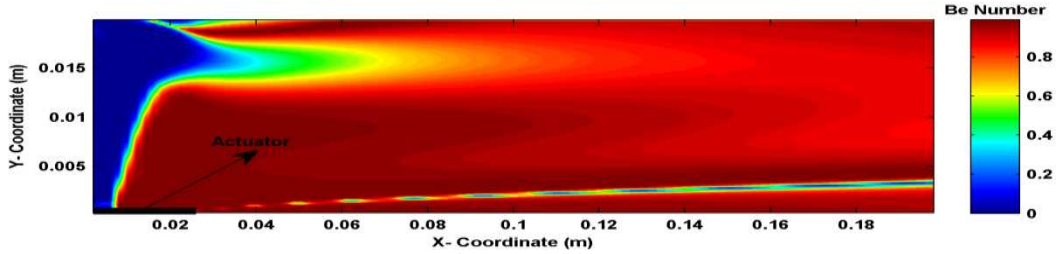

Fig. 14 Bejan number for the case of Maximum Simulated Plasma

Table -3 The Average Entropy Generation Rate in the Computational Domain

Peak Voltage Amplitude (V)	S_{gen} (KW/ m^3K)
1500	0.15
2000	0.23
2500	0.35
3000	0.47
3500	0.59
4000	0.73
4500	0.98
5000	1.16
5500	1.28

Table - 4 The Average Bejan Number in the Computational Domain

Peak Voltage Amplitude (V)	Be
1500	0.54
2000	0.58
2500	0.61
3000	0.65
3500	0.69
4000	0.72
4500	0.75
5000	0.77
5500	0.79

CONCLUSION

DBD plasma based channel flow has been studied in order to the entropy generation rate and Bejan number. Some assumptions have been made during the study. First was to consider the problem two dimensional and incompressible. Ignoring the drift diffusion by the respect of cold plasma formation, allowed us to conduct the present work by modelling the DBD plasma using the Lumped Circuit Element Electro- Static Model. The second assumption was to set the minimum required voltage for ionizing (plasma formation) to be 1KV for all the studied cases. A certain inlet Reynolds number (Re~ 670) with certain geometry of electrodes and channel flow were assumed in this study. The work has been continued by simulating several DBD plasma configurations in which for all cases, applied voltage frequency was set to be 10 KHz and dielectric material was considered to be Kapton with dielectric coefficient of 2.8. So, we changed the actuator configuration by changing the peak voltage amplitude from 1.5 KV to 5.5 KV. The results showed an increase in entropy generation rate by increasing the peak voltage amplitude. Finally, it has been observed that Bejan number does not follow certain behaviour in different applied voltages. So, in the future research we will include the whole engaged parameters in plasma based channel flow and the behaviour of Bejan number will be specifically discussed.

Acknowledgment
Authors are thankful for the great help of Dr. Mani Fathali in fulfilling this research.

REFERENCES

[1] Gad-el-Hak M, Flow Control, Passive, Active and Reactive Flow Management, 1st Ed. Virginia Commonwealth University, Cambridge University Press, **2000**.
[2] EM Braun, FK Lu and DR Wilson, Experimental Research in Aerodynamic Control with Electric and Electromagnetic Fields, Progress in Aerospace Sciences, **2009**, 45, 30-49.
[3] TC Corke, CL Enloe and SP Wilkinson, Dielectric Barrier Discharge Plasma Actuators for Flow Control, *Annual Review of Fluid Mechanics*, **2010**, 42, 505-29.
[4] E Moreau, Airflow Control by Non-Thermal Plasma Actuators, *Journal of Physics D: Applied Physics*, **2007**, 40, 605-636.
[5] LN Cattafesta and M Sheplak, Actuators for Active Flow Control, *Annual Review of Fluid Mechanics*, **2011**, 43, 247-272.
[6] PF Zhang, JJ Wang LH Feng and GB Wang, Experimental Study of Plasma Flow Control on Highly Swept Delta Wing, *AIAA Journal*, **2010**, 48, 249-252.
[7] R Sosa, E Arnaud, E Memin and G Artana, Study of the Flow Induced by a Sliding Discharge, *IEEE Transactions on Dielectrics and Electrical Insulation*, **2009**, 16, 305-311.
[8] DM Orlov, *Modelling and Simulation of Single Dielectric Barrier Discharge Plasma Actuators* [Dissertation], Notre Dame, Indiana, University of Notre Dame, **2006**.
[9] DM Orlov, T Apker, C He, H Othman, TC Corke, Modeling and Experiment of Leading Edge Separation using SDBD Plasma Actuators, *AIAA Paper* No 2007-0877, **2007**.
[10] TC Corke, ML Post and DM Orlov, Single Dielectric Barrier Discharge Plasma Enhanced Aerodynamics, Concepts, Optimization and Applications, *Journal of Propulsion and Power*, **2008**, 24, 935-945.
[11] TC Corke, ML Post and DM Orlov, Single Dielectric Barrier Discharge Plasma Enhanced Aerodynamics, Physics, Modeling and Applications (Review Article), Experimental Fluids, **2009**, 46(1), 1-26.
[12] Habchi Charbel and Antar Ghassan, Direct Numerical Simulation of Electromagnetically Forced Flows using Open FOAM, *Computers and Fluids*, **2015**, 116, 1–9.
[13] Gaitonde V Datta, Analysis of Plasma-based Flow Control Mechanisms through Large-Eddy Simulations, *Computers and Fluids*, **2013**, 85, 19–26.
[14] D. Rizzetta, M. Visbal, Plasma flow control simulations of a low-Reynolds number low-aspect-ratio wing, *Computers and Fluids*, **2012**, 70, 95–114
[15] IH Ibrahim and M Skote, Simulating Plasma Actuators in a Channel Flow Configuration by Utilizing the Modified Suzen–Huang Model, *Computers and Fluids*, **2014**, 99, 144–155.
[16] Zexiang Li, Baopeng Hu, Shilong Lan a, Jinbai Zhang, Junji Huang, Control of Turbulent Channel flow using a Plasma-based Body Force, *Computers and Fluids*, **2015**, 19, 26–36.
[17] M Debiasi and L Jiun-Ming, Experimental Study of a DBD-Plasma Driven Channel Flow, *AIAA Paper*, **2011**, 954.
[18] S Aberoumand, A Jafarimoghaddam and H Aberoumand, Numerical Investigation on the Impact of DBD Plasma Actuators on Temperature Enhancement in the Channel Flow, *Heat Transfer-Asian Research*, **2016**, doi: 10.1002/htj.21227.
[19] BE Mertz, Refinement, Validation and Implementation of Lumped Circuit Element Model for Single Dielectric Barrier Discharge Plasma actuators [Dissertation], USA, University of Notre Dame, **2010**.